Heliyon 9 (2023) e17169

Contents lists available at ScienceDirect

Heliyon

journal homepage: www.cell.com/heliyon

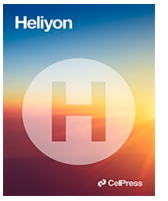

Development of core-shell magnetic molecularly imprinted polymer-based electrochemical sensor for sensitive and selective detection of ezetimibe

Ayemeh Bagheri Hashkavayi [a], Abdolhossein Alizadeh [b], Razieh Azimi [c], Moazameh Peyrovi [d], Jahan Bakhsh Raoof [e], Honggu Chun [a,f,*]

[a] Department of Biomedical Engineering, Korea University, Seoul 02841, South Korea
[b] Department of Chemical Industry, Bushehr Branch, Technical and Vocational University, Bushehr, Iran
[c] Research Institute of Forests and Rangelands, Agricultural Research, Education and Extension Organization (AREEO), Tehran, Iran
[d] Department of Analytical Chemistry, Faculty of Chemistry, University of Mazandaran, Babolsar, Iran
[e] Electroanalytical Chemistry Research Laboratory, Department of Analytical Chemistry, Faculty of Chemistry, University of Mazandaran, Babolsar, Iran
[f] Interdisciplinary Program in Precision Public Health, Korea University, Seoul 02841, South Korea

ARTICLE INFO

Keywords:
Molecularly imprinted polymer
Ezetimibe
Electrochemical sensors
Magnetic nanoparticles
Core-shell structure

ABSTRACT

A sensitive electrochemical molecularly imprinted polymer (MIP) sensor was fabricated for detection of ezetimibe (Eze) as an effective cholesterol absorption inhibitor on the surface of a screen-printed carbon electrode based on a magnetic nanoparticle decorated with MIP (Fe_3O_4@MIP). Placing the magnetic nanoparticle inside the MIP increases the biocompatibility, surface-to-volume ratio, and sensitivity of the sensor. Methacrylic acid (MAA) was used as a monomer, ethylene glycol dimethacrylate (EGDMA) as a cross-linker, and Eze as a template. The fabricated Fe_3O_4@MIP was characterized using Fourier-transform infrared spectroscopy (FTIR), Transmission electron microscopy (TEM), and scanning electron microscopy (SEM). Detection of Eze was achieved by differential pulse voltammetry. Using this sensor, Eze can be sensitively detected in the range of 1.0 nM–10 μM and detection limit of 0.7 nM. In addition, we have shown that the proposed sensor successfully detects different concentrations of Eze in human serum samples and thus proves its practical application.

1. Introduction

Ezetimibe (Eze) is a cholesterol absorption inhibitor drug in the small intestine villi, which leads to a decrease in hepatic cholesterol storage. Also, concomitant use of Eze with statins can significantly reduce the risk of coronary heart disease [1,2]. Measuring very small amounts of compounds in biological samples is a fundamental issue for analytical chemists to assess their balance within the biological fluids since excessive amounts of components may cause various syndromes. Also, the use of various drugs in human daily life is inevitable and the study of the effectiveness of the drug for therapeutic drug monitoring, pharmacological and pharmacokinetic studies require the provision of reliable, rapid, and efficient methods for qualitative and quantitative analysis [3,4].

After oral administration of 10 mg of ezetimibe, it is absorbed within 4–12 h, and the maximum plasma concertation (0.11–0.173

* Corresponding author. Department of Biomedical Engineering, Korea University, Seoul 02841, South Korea.
E-mail address: chunhonggu@korea.ac.kr (H. Chun).

https://doi.org/10.1016/j.heliyon.2023.e17169
Received 6 March 2023; Received in revised form 7 June 2023; Accepted 8 June 2023
Available online 10 June 2023

μmol L^{-1}) occurs 1–2 h post-dose. The final measurable concentration of the drug is approximately 126.01 ± 69.01 nghmL^{-1} [5]. Quality control of the drug has become a rigorous tool in pharmacy to ensure product accurate implementation. Analytical techniques that are mainly used for Eze analysis included UV–Vis spectroscopy, liquid chromatography-mass spectrometry (LCMS), ultra performance liquid chromatography (UPLC), densitometry, electrokinetic chromatography, LC/MS-MS, electrophoresis, and voltammetry [6–9]. Some of these techniques do not show sufficient detection limits or selectivity in diagnosis, are very time consuming due to complex sample preparation and pre-concentration, and require expensive tools of considerable size [10]. The complexity and the very low concentration of drugs in the biological samples make it mandatory to perform preliminary steps of sample preparation before final analysis. Therefore, development of an analytical method, as well as the selection of an appropriate method for the pharmacokinetic evaluation of Eze in humans to quantify drug concentrations in plasma or serum samples taken at different times from individuals can be challenging. Electrochemical methods have been used for the analysis of pharmacological compounds [11,12], these methods offer the advantage of low cost, high sensitivity, and low limit of detection, fast response, direct analysis, and are portable. Therefore, electrochemical methods have become more popular as an alternate method for the analysis of pharmaceutical and biological samples.

Moreover, several signal amplification strategies have been used in electrochemical assays to detect small amounts of target molecules. One of the strategies to amplify the signal and increase the sensitivity is to modify the electrode surface with nanoparticles. Today, magnetic nanoparticles have been used in the fields of separation, catalysis, and biosystems due to their small sizes, high surface to volume ratio, effective and easy separation [13,14]. Magnetic nanoparticles enclosed by molecularly imprinted polymers (MIPs) have the property of selectivity of MIPs in addition to the advantages of magnetic nanoparticles.

MIPs have received a great deal of attention and have been widely used as promising alternatives to bioreceptors in electrochemical sensors [15–17]. MIPs can be synthesized by polymerizing monomers combined with the template (target molecule). In this process, a mixture of functional monomers around a selected target as a template is polymerized, and after the formation of a polymer matrix, the target molecule is released and the carved holes are created, which in terms of the size, molecular shape, and sequence of functional groups are complement with the target molecule and are therefore able to selectively identify the target molecules. The main advantages of MIPs as synthetic receptors are their high selectivity to the target molecule, excellent chemical and thermal stability, their reproducibility and cost-effective preparation [18–20]. The combination of MIPs with a sensor platform in electrochemical methods represents a valuable approach to the development of sensitive sensing systems and is one of the most promising strategies for rapid and selective monitoring of target molecules due to its inherent advantages such as molecular properties, and physicochemical stability in harsh chemical environments. Here, we report the development of a core-shell Fe_3O_4@MIP-based electrochemical sensor by the decoration of methacrylic acid-modified magnetic nanoparticles (core) with molecularly imprinted polymer (shell) for measuring Eze for the first time. The aim of this work is to develop a simple, low-cost, fast, sensitive, and validated method for the determination of Eze without complicated sample preparation or pre-concentration steps.

2. Experimental

2.1. Chemicals and reagents

Potassium hexacyanoferrate (III), potassium hexacyanoferrate (II), polyvinylpyrrolidone (PVP), oleic acid, ferrous chloride tetrahydrate ($FeCl_2{\cdot}4H_2O$), ferric chloride hexahydrate ($FeCl_3{\cdot}6H_2O$), benzoyl peroxide, ethylene glycol dimethacrylate (EGDMA), and methacrylic acid (MAA) were purchased from Sigma Aldrich (Germany). Standard of Eze was kindly supplied by the Dr. Abidi pharmaceutical laboratory Co (Iran).

2.2. Instrumentation

Screen-printed graphite electrodes (SPGEs, 3 mm diameter of working electrode) were obtained from Ecobioservices & Researches (Italy). All voltametric and impedance (EIS) measurements were carried out using Autolab PGstut 30 analyzer controlled by GPES 4.9, and FRA software (Netherlands). Morphology and properties of synthesized Fe_3O_4@MIP were characterized by scanning electron microscopy (SEM) image, FT-IR spectra, and transmission electron microscopy (TEM) image, and the magnetic properties of the MIP which were recorded using Mira 3-XMU FE-SEM (Czech Republic), Shimadzu instrument, TEM-PHILIPS-CM10HT100KV, Vibrating-sample magnetometer-model 155- PAR instrument respectively.

2.3. Synthesis of Fe_3O_4@MIP

Fe_3O_4@MIP was synthesized in two steps:

First, magnetic iron oxide nanoparticles (MNPs) were synthesized through coprecipitation method. For this purpose, 34.6 mmol $FeCl_3{\cdot}6H_2O$ and 17.3 mmol $FeCl_2{\cdot}4H_2O$ were dissolved in 160 ml deionized water. Then 20 ml of ammonium hydroxide solution (25% v/v) was added under the nitrogen atmosphere and 1200 rpm stirring speed at 80 °C. After 1 h the synthesized MNPs were separated by a strong magnet.

In the second step, 1.5 mmol of Eze was dissolved in 10 ml methanol, and 4 mmol of methacrylic acid (MAA) was added and stirred for 30 min (step a). Then, synthesized MNPs (1 g) were mixed with oleic acid (1 ml) and stirred for 15 min (step b). The mixture of the step (a) and ethylene glycol dimethyl acrylate (25 mmol) was added to the mixture of step (b) and placed in an ultrasonic bath for 30 min. In the next step, 0.4 g of polyvinyl pyrrolidine (PVP) as a dispersant was stirred in 100 ml ethanol (80%) at 300 rpm under a

nitrogen atmosphere. The mixture from second step, and 0.1 g of benzoyl peroxide (BPO) as a polymerization initiator were added to the PVP flask. The reaction was carried out at 60 °C for 24 h. After polymerization, the resulting polymer was separated by a strong magnet and washed with a solution of the mixture of methanol/acetic acid (80:20 v/v) under ultrasound, until complete removal of the template molecule. The obtained Fe_3O_4@MIP were washed again with water and dried under vacuum. The magnetic non-imprinted polymers (NIPs) were synthesized by the same method as Fe_3O_4@MIP in the absence of the template molecule [21].

2.4. Fabrication of Fe_3O_4@MIP based sensor for eze detection

As explained in the experimental part, first we synthesized Fe_3O_4@MIP as a selective synthetic capture probe for SPGE surface modification. Then, different concentration (range of 1.0 nM–16 μM) of Eze was dropped (10 μL) onto the electrode surface (Fig. 1). After each step, the modified electrode was thoroughly rinsed with doubly distilled water to remove unbound molecules. The Fe_3O_4@MIP based sensor was then ready to analyze samples containing Eze.

3. Results and discussion

3.1. Structure and morphology analysis of Fe_3O_4@MIP

The synthesis of Fe_3O_4@MIP was verified by the FT-IR method. Fig. 2A shows the FT-IR spectra of (a) Fe_3O_4, (b) Fe_3O_4@MIP, and (c) NIP. The peak at 571 cm^{-1} is related to the Fe–O bond of Fe_3O_4 particles which can be seen in all three spectra and shows the same structure of the synthesized compounds. The peak at about 1200 cm^{-1}, attributable to *C*–O symmetric and asymmetric stretching bands, implied that ethylene glycol dimethacrylate had been loaded onto synthesized structures as cross-linker. The 1720 cm^{-1} bands are arising from the carboxylic groups in MIP and NIP structures. Moreover, the peaks at about 2800–2900 cm^{-1} are ascribed to the C–H asymmetry stretching vibrations. The absorption bands at 3450 cm^{-1} are associated with the O–H vibration. The similarity of the MIP and NIP spectra showed that these polymers have a same structure. In addition, to verify the template removal process, we compared the FT-IR spectra of Eze, Fe3O4@MIP with Eze, and Fe3O4@MIP without Eze in Fig. S1.

In the FT-IR spectrum of Eze (a) absorption peaks at 3247 cm^{-1} (broad O–H stretch), 3009 cm^{-1} (aromatic C–H stretch), 2940 and 2861 cm^{-1} (aliphatic C–H stretch), 1720 cm^{-1} (C═O of lactam), 1602 cm^{-1} (ring skeletal vibration band), 1614, 1508 and 1465 cm^{-1} (ring C═C stretch), 1457 and 1435 cm^{-1} (C–N stretch), 1350 cm^{-1} (in plane O–H bending), 1225 cm^{-1} (C–F stretch), 1116, 1104 and 1061 cm^{-1} (C–O stretch) and 841 cm^{-1} (ring vibration due to para-disubstituted benzene) were observed. After entering the Eze into the MIP, additional peaks appear in the FT-IR spectrum of MIP at 3009 cm^{-1} and 1508 cm^{-1}, which are attributed to aromatic C–H stretching and ring C═C stretching of Eze (b) respectively, while they eliminated in MIP- ezetimibe spectrum by removing of Eze (c).

The morphology and particle size of the synthesized Fe_3O_4@MIP were investigated by SEM and TEM. The SEM image (Fig. 2B) shows that the resulting Fe_3O_4@MIP is porous and has small pores. The polymer adsorption capacity and mass transfer are improved in the presence of these cavities for selective bonding with the analyte. TEM image in Fig. 2C shows Fe_3O_4@MIP spherical shape with particle size about 30 nm. Fig. S2 shows the magnetization curve of synthesized Fe_3O_4@MIP. The magnetic saturation value of Fe_3O_4@MIP is around 9.2 emu g^{-1} indicating that Fe_3O_4@MIP shows superparamagnetic behavior.

3.2. Electrochemical characterization

For the characterization of the Fe_3O_4@MIP modified electrode, the electrochemical cyclic voltammetry (CV) and impedance

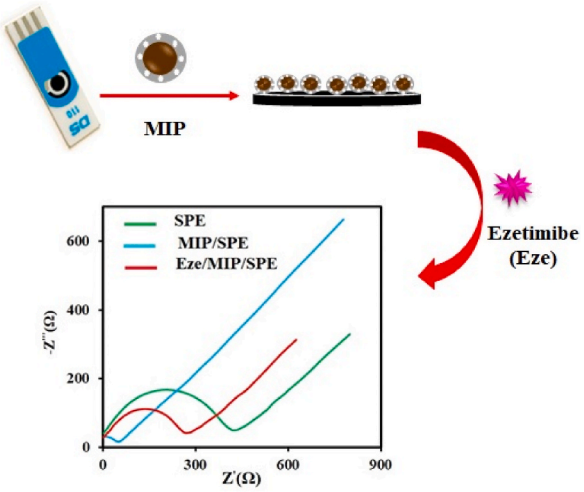

Fig. 1. Schematic illustration of the fabrication of the Fe_3O_4@MIP sensor for Eze detection.

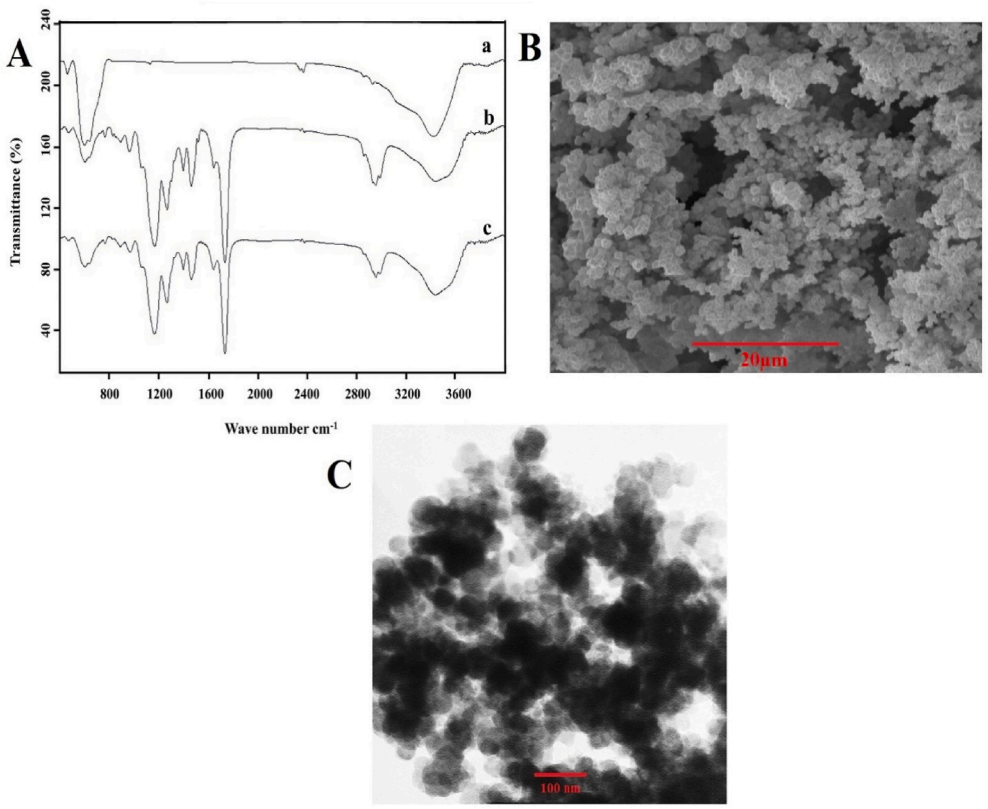

Fig. 2. Characterization of sensing interface. (A) FT-IR spectra of (a) Fe_3O_4 nanoparticles, (b) Fe_3O_4@MIP, and (c) NIP. (B) SEM images of Fe_3O_4@MIP, (**C**) TEM image of MIP.

spectroscopy (EIS, the frequency ranged from 100 kHz to 0.1 Hz at open circuit potential) behaviors of 0.01 M Fe $(CN)_6^{4-/3-}$ redox couple were investigated during the modification steps. As shown in Fig. 3A, Fe $(CN)_6^{4-/3-}$ redox peak currents of Fe_3O_4@MIP modified electrode (curve b) are increased (80 μA) with a with a decrease in ΔEp (0.04 V), compare to the bare SPGE (curve a) (50 μA, ΔEp = 0.27 V) and also in Fig. 3B, when the electrode was modified with Fe_3O_4@MIP, the diameter of the semicircle diminished (curve b) relative to the bare SPGE (curve a). This is due to the high surface area, the porosity of Fe_3O_4@MIP, and high-electron transfer capability which caused an enhancement in the redox peak intensity. The effective surface area of Fe_3O_4@MIP/SPGE was calculated as 0.18 cm^2 using Cottrell equation (chronoamperometry method) which is significantly larger than the bare SPGE (0.07 cm^2) [21]. After incubation of Eze (0.06 μM) with Fe_3O_4@MIP/SPGE, the peak current significantly decreased to 57 μA (Fig. 3 A, curve c) and R_{ct} increased (Fig. 3 B, curve c) because the imprinted cavities are occupied with the target molecules so the accessibility of the redox

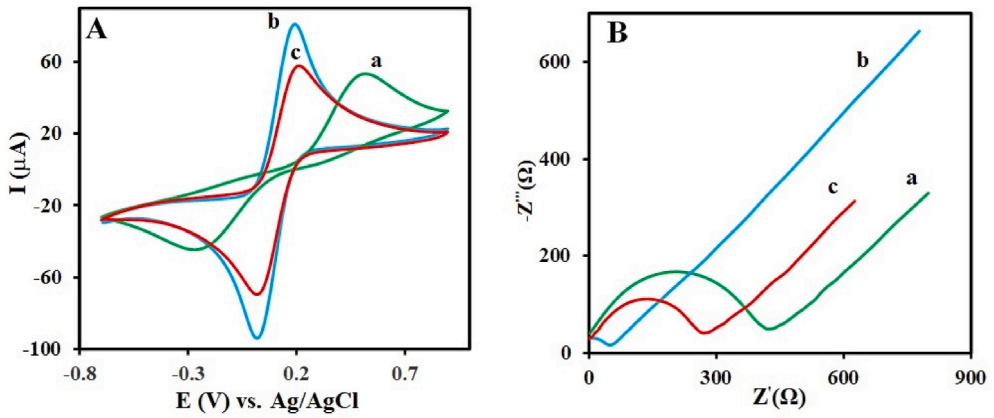

Fig. 3. (A) Cyclic voltammetry (CV), and (B) Nyquist plots of (a) bare SPGE, (b) Fe_3O_4@MIP/SPGE, (c) Eze/Fe_3O_4@MIP/SPGE in 0.01 M $[Fe(CN)_6]^{3-/4-}$ containing 0.1 KCl.

probe to the electrode surface decreased, thus leading to a decrease in electrical conductivity.

3.3. Detection feasibility and optimization of eze sensor

In order to prove the detection feasibility of Fe_3O_4@MIP/SPGE sensor, the differential pulse voltammetry (DPV) method was used to measure oxidation signal of Eze after 8 min of incubation (4 μM) on the surface of bare SPGE (a), NIP/SPGE (b), Fe_3O_4@MIP/SPGE and (c). As shown in Fig. 4, a negligible redox peak current was observed at NIP/SPGE (curve b). After incubation of MIP/SPGE with 1.0 μM Eze, an oxidation peak was observed at 0.51 V in 0.1 M PBS (pH 7.0) (curve c), indicating that Eze was successfully detected by MIP. The affection of Eze incubation time on the fabricated sensor was investigated by the differential pulse voltammetry (DPV) with the potential range from 0.25 to 0.75 V in 0.1 M PBS (pH 7.0). The DPV results indicated that the 8 min incubation time caused to capture more Eze on the Fe_3O_4@MIP/SPGE surface (Fig. S3) and further incubation time did not significantly influence the variation.

3.4. Sensitivity of the proposed sensor and determination of eze in human serum sample

To assess the sensitivity of Fe_3O_4@MIP/SPGE to Eze, we investigate the effect of Eze concentration on DPV response of the fabricated sensor in 0.1 M PBS (pH 7.0). As the concentration of Eze increased, the DPV current at 0.51 V increased gradually (Fig. 5), due to the increase in the number of imprinted holes filled by the Eze. A linear relationship was achieved from 1.0 nM to 10 μM with a limit of detection of 0.7 nM which is superior to previously reported methods for determination of Eze (Table 1). Moreover, another important parameter used to describe the analytical performance of the MIP-based sensors is the imprinting factor, which indicates the detection performance of the fabricated sensor. The imprinting factor, calculated from the slope ratio of calibration plots obtained for both MIP and NIP-modified electrodes [22] (Fig. S4) is equal to 20, thus confirming successful imprinting. The higher DPV current at MIP/SPGE compared to NIP/SPGE, is due to the successfully created specific binding sites leading to selective binding to EZe molecules.

In order to prove the capability of the sensor to measure the Eze in the real sample matrix, known concentrations of Eze were added to the healthy human serum (50% diluted, provided by sigma Aldrich). Analysis and recovery experiments were carried out using our proposed Fe_3O_4@MIP- based sensor, and the results are shown in Table S1. The results showed satisfactory recovery in the range of 101–114% with RSDs (relative standard deviations) of less than 1.5% for Eze determination.

3.5. Selectivity, reproducibility and stability of the sensor

To investigate the selectivity of the Fe_3O_4@MIP/SPGE electrochemical sensor, studies were carried out with atorvastatin and simvastatin as two medicines structurally related to lipid reducing. As shown in Fig. 6, at the equal concentration of each analyte (4 μM), the decrease of the peak current of atorvastatin (Atr), and simvastatin (Sim) is more evident compared to Eze. The results in Fig. 6 shows that the nonspecific interactions of the Fe_3O_4@MIP- based sensor with other analytes are very low (0.005–0.008 μA) compared to Eze (The Eze signal intensity is approximately 12 times that of others). The response of the NIP-based sensor was obviously low compared to all analytes which is mainly due to the non-specific compound adsorption on the polymer surface. It is clear that the detection specificity of the Fe_3O_4@MIP/SPGE sensor to Eze was significantly higher than the rest which can be ascribed to the three-dimensional created cavities in the Fe_3O_4@MIP, which are complementary and well matched to the molecular shape and direction of functional groups of Eze.

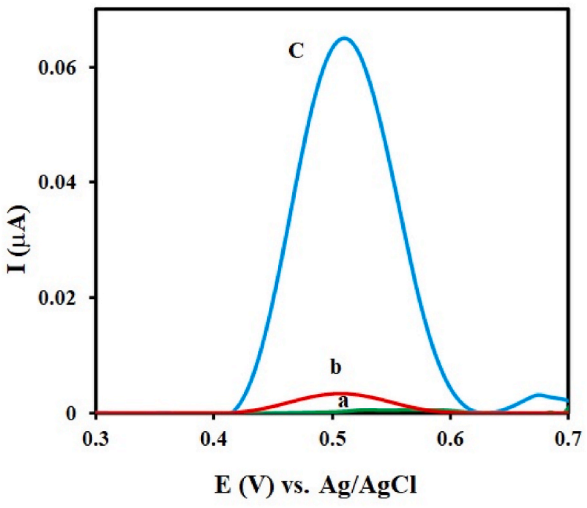

Fig. 4. DPV signals of (a) bare SPGE, (b) NIP/SPGE, and (c) Fe_3O_4@MIP/SPGE after incubation for 8 min with 1.0 μM Eze in 0.1 M PBS (pH 7.0).

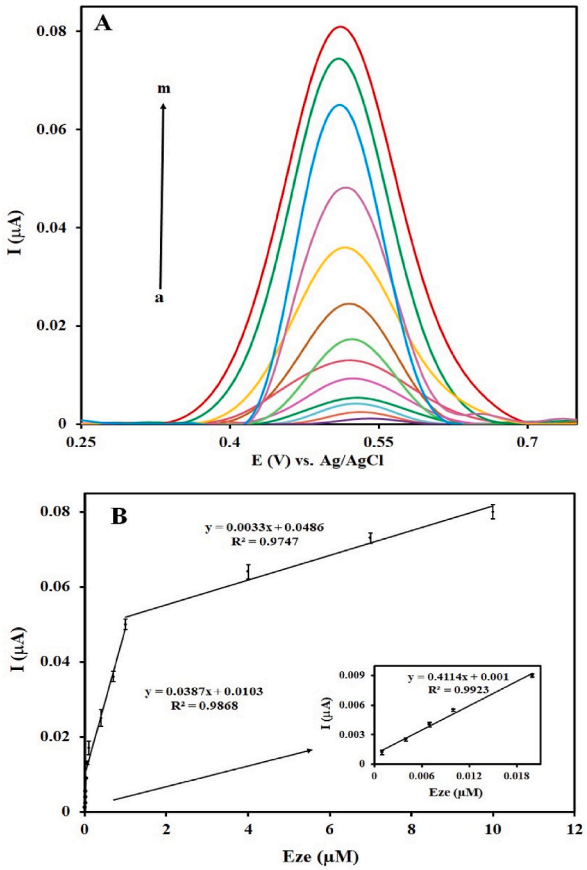

Fig. 5. **(A)** DPV signal response toward various concentrations of Eze: (a) 0.001, (b) 0.004, (c) 0.007, (d) 0.01, (e) 0.02, (f) 0.06, (g) 0.1, (h) 0.4, (i) 0.7, (j)1.0, (k) 4.0, (l) 7.0, and (m) 10 μM in 0.1 M PBS (pH 7.0). (B) Linear relationship between DPV signal changes and the Eze (μM) concentrations.

Table 1
Comparative analysis of different methods for Eze detection.

Detection method	Linear range (mol L^{-1})	Limit of detection (mol L^{-1})	Ref.
DPV	2.0×10^{-7} - 1.0×10^{-5}	5.0×10^{-8}	[23]
AdSV[a]	8.0×10^{-8} - 1.4×10^{-6}	2.8×10^{-8}	[24]
LC–MS/MS[b]	1.0×10^{-8}-97×10^{-8}	1.0×10^{-8}	[25]
HPLC[c]	1.0×10^{-6} - 1.0×10^{-4}	…	[26]
AdSV	4.0×10^{-7}- 7.6×10^{-6}	1.5×10^{-7}	[27]
GC-MS[d]	3.7×10^{-8}–6.0×10^{-7}	2.0×10^{-8}	[28]
DPV	1.0×10^{-9}- 10×10^{-6}	1.0×10^{-9}	This work

[a] Adsorptive stripping voltammetry.
[b] Liquid chromatography-tandem mass spectrometry.
[c] High-performance liquid chromatography.
[d] Gas chromatography-mass spectrometry.

The reproducibility of developed method was evaluated to detect 0.7 μM Eze on 8 prepared Fe_3O_4@MIP/SPGE sensor. The RSD of 1.7% was obtained, reflecting a good sensor-to-sensor reproducibility. To investigate the stability of the sensor a series of 21 Fe_3O_4@MIP/SPGE sensors was fabricated and once every two weeks the prepared sensors were tested by incubating with 0.7 μM Eze. After 10 weeks, it was observed that the as-prepared sensors lost about 6% of initial current, indicating the prepared sensor have excellent long-term stability (Fig. S5).

4. Conclusion

In this study, an electrochemical sensor-based core-shell Fe_3O_4@MIP structure was developed for selective detection of Eze. The

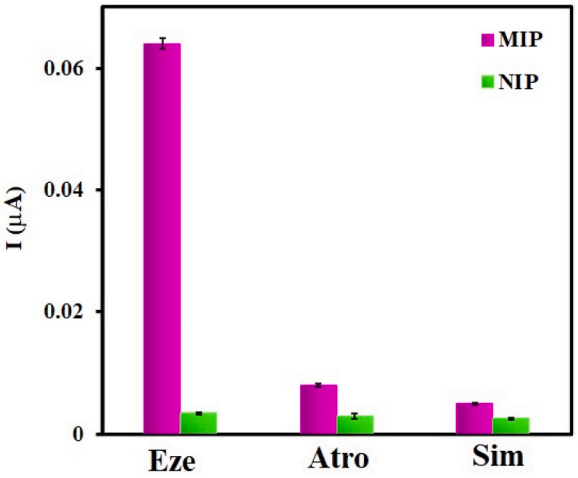

Fig. 6. Selectivity investigation of the prepared sensor to Eze by comparing it with Atorvastatin, and Simvastatin in PBS (0.1 M, pH 7.0).

magnetic nanoparticles were used to improve the effective surface area and sensitivity of the fabricated sensor. Engraved cavities in the polymer provide specific sites for selective detection of Eze via hydrogen bonds. CV, EIS, and DPV techniques have been used for monitoring the interaction between the Fe_3O_4@MIP and Eze. According to the calibration curve of the sensor, it presented a good linear relationship with Eze concentrations in the range of 1.0 nM–10 μM, which was much better than that in most of the detecting methods. In addition, the prepared sensor when applied to detect different concentrations of spiked Eze in human healthy serum samples showed satisfying recovery. The fabricated sensor displayed many attractive features: very easy preparation, simplicity, rapidity, cheapness, high selectivity, and sensitivity in detecting Eze with low detection limit. Future research should focus on the development of MIP-based sensors suitable for being tested in undiluted biological environments. Also, device portability needs to be investigated, where optimal portability is often equipped with miniaturized electrodes and a hand-held analyzer for data processing.

Author contribution statement

Ayemeh Bagheri Hashkavayi: Conceived and designed the experiments; Performed the experiments; Analyzed and interpreted the data; Wrote the paper.

Abdolhossein Alizadeh: Performed the experiments; Analyzed and interpreted the data.

Razieh Azimi: Analyzed and interpreted the data.

Moazameh Peyrovi: Performed the experiments.

Jahan Bakhsh Raoof: Contributed reagents, materials, analysis tools or data.

Honggu Chun: Analyzed and interpreted the data; Contributed reagents, materials, analysis tools or data; Wrote the paper.

Data availability statement

Data will be made available on request.

Declaration of competing interest

The authors declare that they have no known competing financial interests or personal relationships that could have appeared to influence the work reported in this paper

Acknowledgements

This research was supported by the National Research Foundation of Korea (NRF) (NRF-2018M3A9D7079485 and NRF-2020R1A2C3010322).

Appendix A. Supplementary data

Supplementary data to this article can be found online at https://doi.org/10.1016/j.heliyon.2023.e17169.

References

[1] J.J.M. Nasr, N.H. Al-Shaalan, S.M. Shalan, Sustainable environment-friendly quantitative determination of three anti-hyperlipidemic statin drugs and ezetimibe in binary mixtures by first derivative Fourier transform infrared (FTIR) spectroscopy, Spectrochim. Acta Mol. Biomol. Spectrosc. 237 (2020), 118332.
[2] D. Zodda, R. Giammona, S. Schifilliti, Treatment strategy for dyslipidemia in cardiovascular disease prevention: focus on old and new drugs, Pharmacy 6 (1) (2018) 10.
[3] H. Danafar, M. Hamidi, A rapid and sensitive LC–MS method for determination of ezetimibe concentration in human plasma: application to a bioequivalence study, J. Chromatogr., A 76 (23–24) (2013) 1667–1675.
[4] A. Bergman, et al., Assessment of pharmacokinetic interactions between ezetimibe and cyclosporine, Clin. Pharmacol. Therapeut. 77 (2) (2005) P75.
[5] N.-N. Chu, et al., Pharmacokinetics and safety of ezetimibe/simvastatin combination tablet: an open-label, single-dose study in healthy Chinese subjects, Clin. Drug Invest. 32 (2012) 791–798.
[6] D.Ş. Özden, Z. Durmuş, E. Dinç, Electrochemical oxidation behavior of ezetimibe and its adsorptive stripping determination in pharmaceutical dosage forms and biological fluids, Res. Chem. Intermed. 41 (3) (2015) 1803–1818.
[7] K. Attia, M. Nassar, A. Abdelfattah, Bivariate and multivariate spectrophotometric methods for determination of ezetimibe with kinetic study of its alkaline degradation, J. Anal. Pharm. Res. 3 (4) (2016) 42–54.
[8] S. Li, et al., Liquid chromatography–negative ion electrospray tandem mass spectrometry method for the quantification of ezetimibe in human plasma, J. Pharm. Biomed. 40 (4) (2006) 987–992.
[9] M. Attimarad, Capillary electrophoresis method development for simultaneous determination of atorvastatin and ezetimibe from solid dosage form, J. Young Pharm. 9 (1) (2017) 120.
[10] S. Chitravathi, S. Reddy, E.C. Swamy, Electrochemical determination of ezetimibe by MgO nanoflakes-modified carbon paste electrode, J. Electroanal. Chem. 764 (2016) 1–6.
[11] A. Bagheri Hashkavayi, J.B. Raoof, R. Ojani, Preparation of epirubicin aptasensor using curcumin as hybridization indicator: competitive binding assay between complementary strand of aptamer and epirubicin, Electroanalysis 30 (2) (2018) 378–385.
[12] L. Fotouhi, A. Bagheri Hashkavayi, M.M. Heravi, Electrochemical behaviour and voltammetric determination of sulphadiazine using a multi-walled carbon nanotube composite film-glassy carbon electrode, J. Exp. Nanosci. 8 (7–8) (2013) 947–956.
[13] A. Bagheri Hashkavayi, J.B. Raoof, K.S. Park, Sensitive electrochemical detection of tryptophan using a hemin/G-quadruplex aptasensor, Chemosensors 8 (4) (2020) 100.
[14] F. Mollarasouli, et al., Magnetic nanoparticles in developing electrochemical sensors for pharmaceutical and biomedical applications, Talanta 226 (2021), 122108.
[15] B. Feier, et al., Electrochemical sensor based on molecularly imprinted polymer for the detection of cefalexin, Biosensors 9 (1) (2019) 31.
[16] A. Raziq, et al., Development of a portable MIP-based electrochemical sensor for detection of SARS-CoV-2 antigen, Biosens. Bioelectron. 178 (2021), 113029.
[17] D. Dechtrirat, et al., An electrochemical MIP sensor for selective detection of salbutamol based on a graphene/PEDOT: PSS modified screen printed carbon electrode, RSC Adv. 8 (1) (2018) 206–212.
[18] O.S. Ahmad, et al., Molecularly imprinted polymers in electrochemical and optical sensors, Trends Biotechnol. 37 (3) (2019) 294–309.
[19] F. Zouaoui, et al., Electrochemical sensors based on molecularly imprinted chitosan: a review, TrAC, Trends Anal. Chem. (2020), 115982.
[20] N. Leibl, et al., Molecularly imprinted polymers for chemical sensing: a tutorial review, Chemosensors 9 (6) (2021) 123.
[21] M. Peyrovi, M. Hadjmohammadi, I. Saeidi, Synthesis of magnetic nanoparticle-based molecularly imprinted polymer as a selective sorbent for efficient extraction of ezetimibe from biological samples, Biomed. Chromatogr. 33 (1) (2019), e4404.
[22] V. Ayerdurai, et al., Electrochemical sensor for selective tyramine determination, amplified by a molecularly imprinted polymer film, Bioelectrochemistry 138 (2021), 107695.
[23] S. Chitravathi, S. Reddy, B.K. Swamy, Electrochemical determination of ezetimibe by MgO nanoflakes-modified carbon paste electrode, J. Electroanal. Chem. 764 (2016) 1–6.
[24] M.L. Yola, N. Özaltin, Adsorptive stripping voltammetric methods for determination of ezetimibe in tablets, Rev. Anal. Chem. 30 (1) (2011) 29–36.
[25] M.S. Babu, et al., Development and validation of a high-throughput LC-MS/MS method for the quantitation of total ezetimibe in human plasma, Int. J. Pharmaceut. Sci. Rev. Res. 39 (2016) 338–345.
[26] R. Sistla, et al., Development and validation of a reversed-phase HPLC method for the determination of ezetimibe in pharmaceutical dosage forms, J. Pharm. Biomed. 39 (3–4) (2005) 517–522.
[27] D.Ş. Özden, Z. Durmuş, E. Dinç, Electrochemical oxidation behavior of ezetimibe and its adsorptive stripping determination in pharmaceutical dosage forms and biological fluids, Res. Chem. Intermed. 41 (3) (2015) 1803–1818.
[28] E. Uçaktürk, N. Özaltin, B. Kaya, Quantitative analysis of ezetimibe in human plasma by gas chromatography-mass spectrometry, J. Separ. Sci. 32 (11) (2009) 1868–1874.